Hydrogenation behavior of Ti–44Al–6Nb alloy and its effect on the microstructure and hot deformability

Tengfei Ma, Ruirun Chen,[a] Deshuang Zheng, Chang Liu, Jingjie Guo, Hongsheng Ding, Yanqing Su, and Hengzhi Fu
School of Materials Science and Engineering, Harbin Institute of Technology, Harbin 150001, China

(Received 7 October 2016; accepted 20 December 2016)

The hydrogenation behavior of Ti–44Al–6Nb (at.%) alloy was studied at temperature range of 1373–1693 K, and the effect of hydrogen on hot deformability was tested on Gleeble-1500D thermo-simulation machine. It is found that the $\ln C_H$ increases linearly with $1/T$, and hydrogen content increases with increasing of hydrogen time and flow rate logarithmically. The positive heat of solution of hydrogen denotes that hydrogen absorption in TiAl alloys is an endothermic reaction. The results also show that hydrogen promotes the lamellar colony size and lamellar spacing because that hydrogen can promote the diffusion of elements. There is more residual B2 phase in the hydrogenated alloy revealing that hydrogen stabilizes the B2 phase during hydrogenation. The nanohardness and elastic modulus of the alloy are decreased from 4.4 and 213.5 GPa to 4.2 and 199.8 GPa after hydrogenation with 0.033 wt% H. Thermal simulation results show that the peak stress is decreased by 30% after hydrogenation with 0.033 wt% H which corresponds to decreasing the deformation temperature by about 50 K. This is attributed to hydrogen-promoted dynamic recrystallization and dislocation movement.

I. INTRODUCTION

TiAl alloys have attractive mechanical properties such as, high specific strength, excellent oxidation resistance, and good creep resistance which are considered the most potential materials for replacement of nickel based alloys and refractory alloys at temperature range of 973–1223 K.[1,2] The coexistence of covalent bond and metallic bond in the TiAl alloys results in poor ductility and high deformation resistance. The ductility of TiAl alloys is less than 1% at room temperature which is the main barriers for their application.[3,4] The peak stress of Ti–45Al–(8–9)Nb–(W, B, Y) alloy is 240 MPa deformed at 1423 K under strain rate of 0.05 s^{-1} resulting in difficult deformation.[5]

Thermohydrogen processing (THP) is a new method that hydrogen is used as a temporary element to control the microstructure and improve the hot workability of titanium alloys, α_2-based alloys.[6–8] The studies show that the microstructure can be refined by hydrogen-induced phase transformation and the flow stress can be decreased because that hydrogen can promote the dynamic recrystallization and dislocation movement, e.g., the stress of Ti–6Al–4V alloy is decreased by 11.2% and the plasticity is increased by 20% after addition of 0.3 wt% H.[9] The THP of TiAl alloys has been studied recently, the researches are mainly focus on the effect of hydrogen on hot deformation of TiAl alloys.[10,11] The peak stress of Ti–46Al–2V–1Cr–0.3Ni alloy is decreased by approximately 35% when deformed at 1423 K and 0.001 s^{-1}. However, the hydrogenation behaviors of the alloys are short of systematic research. The THP process of titanium alloy is directly applied to TiAl alloys, such as the hydrogenation temperature of Ti–46Al–2V–1Cr–0.3Ni alloy is 973 K which is often used in titanium alloy. The low solubility of hydrogen in TiAl alloys (nearly zero at room temperature) restricted the application of THP to TiAl alloys, which was reported by Takasaki.[12] Takasaki[13,14] also attempted to improve the solubility of hydrogen in TiAl alloys by enhancing the temperature (843 K) and hydrogen pressure (10 MPa). The results show that hydrogen absorption in TiAl alloys is an endothermic reaction, hydrogen uptake increases with increasing of temperature (94.1 wppm at 723 K and 347.2 wppm at 823 K for Ti44Al alloy) and pressure (10 at% for Ti45Al alloy at 923 K under 10 MPa). It is considered that hydrogen content increases with increasing of temperature and temperature can promote hydrogen absorption in TiAl alloys. The microstructural evolution of TiAl alloys during high temperature is complicated because of the complicated phase transition such as $\alpha \rightarrow (\alpha/\gamma)_L \rightarrow (\alpha_2/\gamma)_L$, $\alpha \rightarrow \gamma$.[15–18] Various microstructures can be achieved by controlling the heating temperature, soaking temperature, and cooling rate, e.g., duplex microstructure, nearly microstructure and massive γ phase. Hydrogen can decrease the beta-transus

Contributing Editor: Jürgen Eckert
[a]Address all correspondence to this author.
e-mail: ruirunchen@hit.edu.cn
DOI: 10.1557/jmr.2016.520

 © Materials Research Society 2017

https://doi.org/10.1557/jmr.2016.520 Published online by Cambridge University Press

temperature of titanium alloy and hydrogen is beta stabilizing element, which will have a great effect on the microstructures and phases of TiAl alloys.[19] As a result, the microstructural evolution of TiAl alloys during gaseous hydrogen charging at high temperature becomes more complicated because of the co-effect of hydrogen and heat treatment. The present study focus on the hydrogenation behavior of TiAl alloys at different conditions, temperature ranges from 1373 to 1693 K, hydrogenation time varied from 10 to 60 min and hydrogen flow rate was changed from 20 to 200 mL/min. The effect of hydrogen on microstructural evolution was observed after hydrogenation at different temperatures, and the effect of hydrogen on the hot workability was tested at temperature range from 1373 to 1523 K under strain rate of 0.01 s^{-1}.

II. EXPERIMENTAL PROCEDURE

The materials used in this study with nominal composition of Ti–44Al–6Nb alloy were prepared by vacuum self-consuming arc melting. The samples used for hydrogenation were cut from the center of the ingot using wire-electrode cutting. The size of the samples is Φ 8 × 12 mm. The surface was mechanical ground by P 2000 sandpaper and then ultrasonically cleaned by ethanol solution. The hydrogenation was carried out on a vacuum furnace which could be heated to 1873 K and the ultimate vacuum degree is 1 Pa. To study the effect of temperature on hydrogen absorption, the samples were heated to target temperature (1373, 1473, 1553, 1623 and 1693 K) in hydrogen atmosphere and soaked for 60 min to ensure that hydrogen permeation in TiAl alloys is complete. The furnace was evacuated and then filled with argon atmosphere before heating. This process was repeated for three times to eliminate the oxygen. The effect of hydrogen flow rate and hydrogenation time on hydrogen absorption was investigated under different temperatures. The samples were heated to target temperature in argon atmosphere, then a steady flow of pure hydrogen with hydrogen flow rate range from 20 to 200 mL/min was flowed in and maintained for different time (10, 20, 30, and 60 min). The hydrogen flow rate was controlled by a flowmeter. The hydrogen content was determined by weighting the samples before and after hydrogenation using a high accuracy balance with accuracy of 10^{-4} g. Each sample was weighted three times and the final results were the average. The hydrogen content was calculated into weight percent. The H–O analysis was carried out on LECO-ROH600 oxygen/hydrogen analyzer for accurate measurement of hydrogen content and oxygen content. The size of the specimens was Φ 3 × 4 mm and the final result was the average of 3 tested results. The isothermal heat treatment was carried out under argon atmosphere for comparison to eliminate the effect of heat treatment. The samples after hydrogenation and isothermal heat treatment at 1473 K were selected for mechanical properties test and the hydrogen content was controlled by hydrogen flow rate.

The phase transformation temperature of Ti–44Al–6Nb alloy was determined by quenched microstructures and differential scanning calorimetry (DSC). The samples were heated to 1573 K and soaked for 60 min, then were quenched into water every 10 K until to 1513 K. The DSC experiment was carried out from room temperature up to 1723 K at a heating rate of 10 K/min on NETZSCH STA 449F3. The test was performed under a dynamic argon atmosphere with a flow rate of 40 mL/min.

The nanohardness was tested on Nano Indenter XP machine, the indenter pressed on the surface of the samples with depth of 800 nm and the internal of the lamellar colony was selected, the result was the average of 5 points. The thermo-compression was carried out on Gleeble-1500D thermo-simulation machine under temperature range of 1373–1523 K and strain rate of 0.01 s^{-1}, the engineering strain of the specimen was 0.6 (≈0.8 true strain). The Pt–Rh thermocouple was used to monitor the temperature during the experiment. The samples were quenched to water after compression to reserve the hot deformation microstructure.

The microstructures of unhydrogenated and hydrogenated Ti–44Al–6Nb alloys were investigated by optical microscope (OM), and the size of lamellar colony was measured by quantitative metallography method. The samples were ground, polished, and then etched by a Kroll solution (10 vol% HNO_3 + 10 vol% HF + 80 vol% H_2O). The microstructure was further analyzed by scanning electron microscope (SEM) and transmission electron microscope (TEM). The TEM specimens were ground by about 80 μm in thickness and then were twin-jet polished with a solution of 6 vol% perchloric acid + 34 vol% butanol + 60 vol% methanol (6% $HClO_4$ + 60% CH_3OH + 34% $CH_3(CH_2)_3OH$) at about −20 °C and 25 V. The phase of unhydrogenated alloy and hydrogenated alloy was studied by X-ray diffractometer (XRD, D/max-rB) with the 2θ scan ranging from 20 to 90° at a speed of 5°/min.

III. RESULTS AND DISCUSSION

A. Original microstructure

The microstructure of as-cast Ti–44Al–6Nb alloy is dendrite structure and the B2 phase distributes inhomogeneously as shown in Fig. 1(a). The bright microstructure is the B2 phase and the dark regions are the Al-segregation, which can be observed in TiAl alloys after addition of beta stabilizing elements. The B2 phase and Al-segregation are formed during the solidification due to the different equilibrium solute partition coefficient of

https://doi.org/10.1557/jmr.2016.520 Published online by Cambridge University Press

Nb and Al elements.[20] The lamellar spacing is about 500 nm based on statistics of several TEM images. However, the B2 phase is not observed, which is common seen in TiAl alloys after addition of high content of beta stabilizing elements.[21] This is because that the Nb content is low and little B2 phase is formed.

B. Determination of phase transformation point

Before hydrogenation, the α-transu temperature (T_α) of Ti–44Al–6Nb alloy is determined by quenched microstructures and DSC as shown in Fig. 2. The T_α (T_α; reaction $\gamma \rightarrow \alpha$) is determined to be 1523–1533 K based on the quenched microstructures. The DSC result shows that the T_α is 1529.9 K. The T_{eu} (T_{eu}; reaction $\alpha_2 + \gamma \rightarrow \alpha$) transformation temperature is not obvious as shown in the DSC curves. The T_{eu} temperature is determined to be about 1433 K by referencing the results of H. Clemens.[22] The hydrogenation temperature (1373, 1473, 1553, 1623, and 1693 K) is selected based on the phase transition temperature. The hydrogenation temperature is designed to be located at different phase regions,

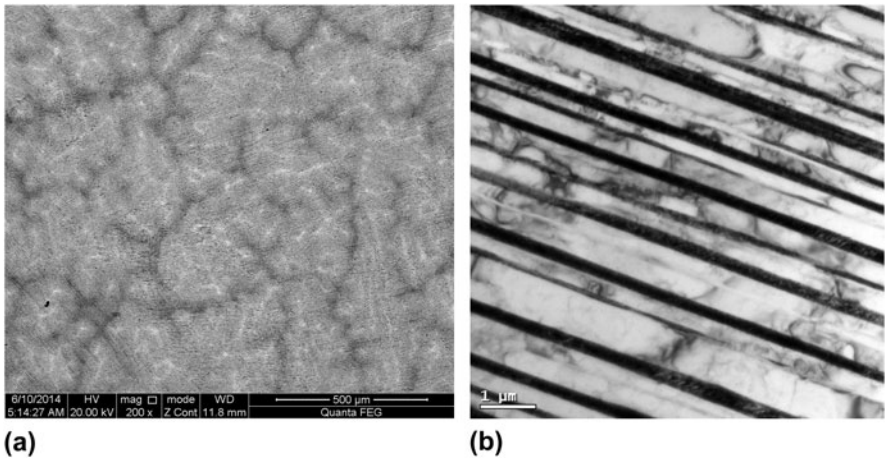


FIG. 1. Microstructure of as-cast Ti–44Al–6Nb alloy: (a) microstructure by SEM-BSE, (b) TEM image of lamellar.

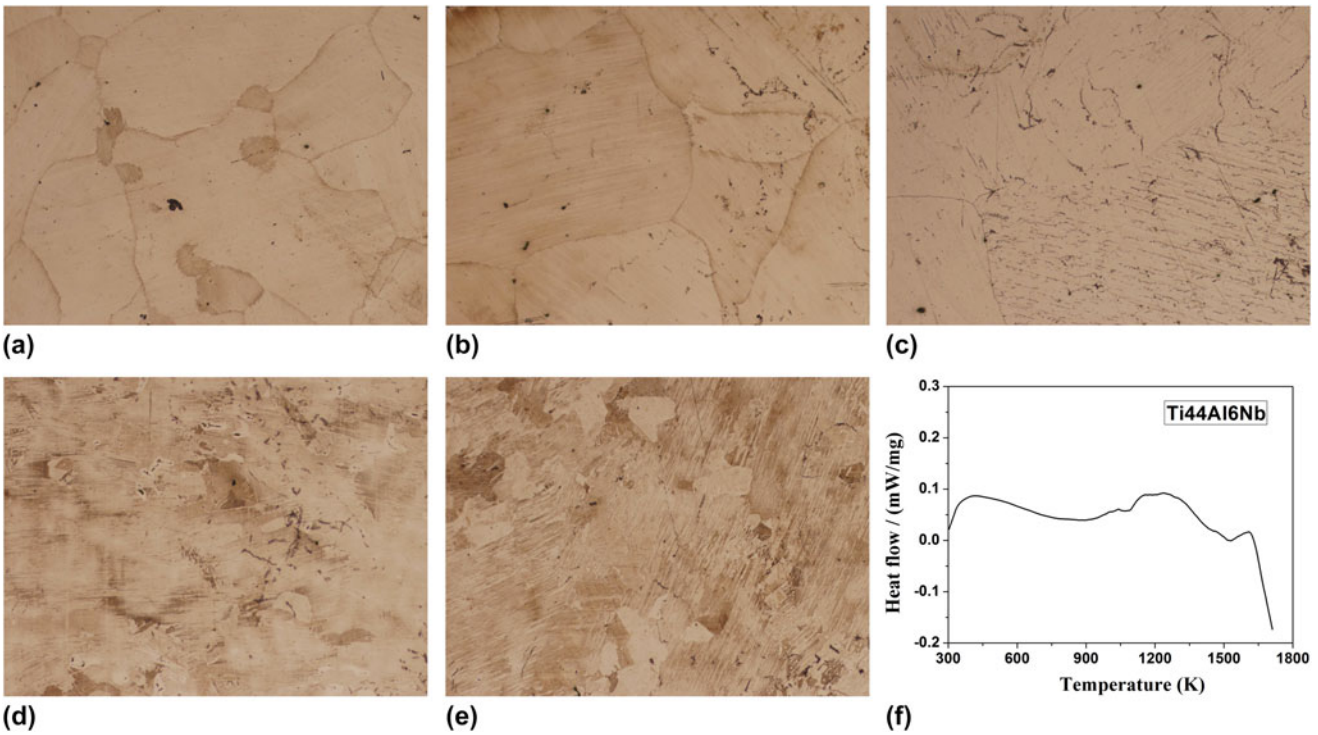


FIG. 2. Quenched microstructures and DSC curve of Ti–44Al–6Nb alloy: (a) 1513 K; (b) 1523 K; (c) 1533 K; (d) 1543 K; (e) 1553 K; (f) DSC curve.

https://doi.org/10.1557/jmr.2016.520 Published online by Cambridge University Press

such as 1373 K is located in the $\alpha_2 + \gamma$ phase region and 1553 K is located in the single α phase region.

C. Hydrogen absorption at high temperature

The effect of temperature on hydrogen content is shown in Fig. 3. Hydrogen content increases with increasing of temperature, the maximum hydrogen content is about 0.089 wt% at 1693 K, which is about three times than that at 1373 K. Hydrogen content is also influenced by different phases because of the different crystal structures, the maximum solubility of hydrogen in α_2 is larger than that in γ phase based on the first-principles calculation and experimental results.[13,23] Although the hydrogen absorption behavior of B2 phase is unknown, it is considered that B2 phase can absorb hydrogen because that the B2 phase is BCC structure. With increasing of temperature, the B2 phase dissolves and the γ phase transforms to α phase leading to hydrogen absorption complicate. Hydrogen content is determined by temperature and the crystal structure of different phase. Figure 3 exhibits that there is a linear relationship between lnC and l/T. The relationship between hydrogenation temperature and hydrogen content fits with the Arrhenius equation which is written as below[12,24,25]:

$$C_{\mathrm{H}} = KP_{\mathrm{H_2}} \exp(-Q/2RT) \quad , \qquad (1)$$

where C_{H} is the hydrogen content, K is constant depends on the nature of material. $P_{\mathrm{H_2}}$ is the hydrogen pressure, Q is heat of solution of hydrogen in the alloy, R is gas constant, and T is the temperature. From the fitting curve, the Q is calculated to be 81.4 kJ/mol at temperature range of 1373–1693 K. The calculated Q is larger than that of Ti–45Al alloy (58.3 kJ/mol) at the temperatures range of 723–843 K, and the heat of solution of hydrogen in different phases is listed in Table I for comparison.[12] The heat of solution of hydrogen in TiAl alloys is influenced by alloy composition, different phases, hydrogenation temperature, and the preparation method. The positive Q reveals that hydrogen absorption in TiAl alloys is an endothermic reaction and high temperature contributes to hydrogen absorption. The relationship between hydrogen content and hydrogenation temperature is obtained and shown in Eq. (2).

$$C_{\mathrm{H}} = 25.44 \exp\left(-9.792 \times 10^3/T\right) \quad . \qquad (2)$$

The hydrogen content was tested accurately by LECO-ROH600 oxygen/hydrogen analyzer as shown in Fig. 4. The hydrogen content and oxygen content is 0.083 and 0.015 wt% respectively at 1693 K. The hydrogen content is a little lower than that of 0.089 wt% tested by weighting because that oxygen permeation in Ti–44Al–6Nb alloy is easier at high temperature. The results show that hydrogen content obtained by weighting is accurate and believable.

Hydrogenation time is another important parameter to hydrogen absorption, which ensures hydrogen absorption completely. The effect of hydrogenation time on hydrogen content is shown in Fig. 5. Hydrogen content increases with increasing of hydrogenation time logarithmically. The alloy absorbs hydrogen fast at initial stage and then tends to the equilibrium after hydrogenation 30 min indicating that hydrogen absorption is complete within 30 min. The diffusion coefficient of hydrogen in TiAl alloys is 2.6×10^{-10} cm^2/s at room temperature determined by electrolytic charging, it takes about 17.5 h

TABLE I. Heat of solution of hydrogen in different phases.

Alloy	Phase	Heat of solution (kJ/mol)	Temperature (K)
Ti–45Al	$\alpha_2 + \gamma$	58.3	723–843
Ti–50Al	γ	29.4	723–933
Ti–Al(powder)	α_2	141.0	700–811
Ti–44Al–6Nb	$\alpha_2 + \gamma$ + B2	81.4	1373–1693

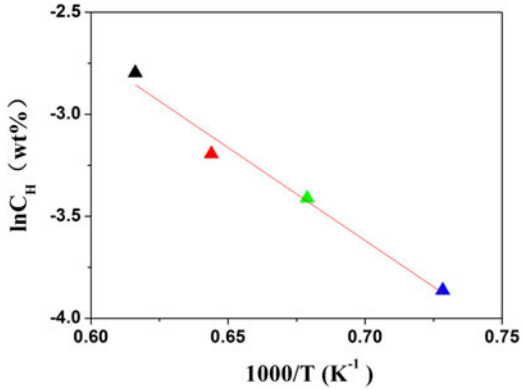


FIG. 3. Plot of lnC versus l/T for the Ti–44Al–6Nb alloy.

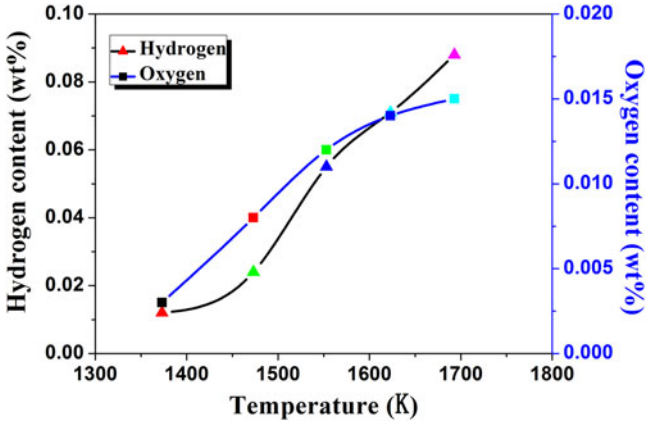


FIG. 4. H-O analysis of Ti–44Al–6Nb alloy at different temperature.

https://doi.org/10.1557/jmr.2016.520 Published online by Cambridge University Press

to uptake completely in TiAl alloys with the size of Φ 8 × 12 mm at room temperature.[26] The diffusion coefficient of hydrogen in Ti–45Al melt is about 5.5 × 10^{-3} cm^2/s as reported by Su,[27] the hydrogenation process will be completed in 100 s. The diffusion coefficient increases with increasing of temperature based on the thermodynamics and our previous study, thus it is possible that TiAl alloys is saturated with hydrogen within 30 min at high temperature (1373–1693 K).

The effect of hydrogen flow rate on hydrogen content at hydrogenation temperature of 1553 K and hydrogenation time of 30 min is shown in Fig. 6. Hydrogen content increases with increasing of hydrogen flow rate firstly and then reaches the equilibrium when the hydrogen flow rate reaches to 100 mL/min. Hydrogen content under hydrogen flow rate of 100–200 mL/min is 0.048 and 0.051 wt% at 1553 K respectively. Consequently, the gaseous hydrogen charging of TiAl alloys is considered to be that hydrogenation time is 30 min and hydrogen flow rate is 100 mL/min at high temperature.

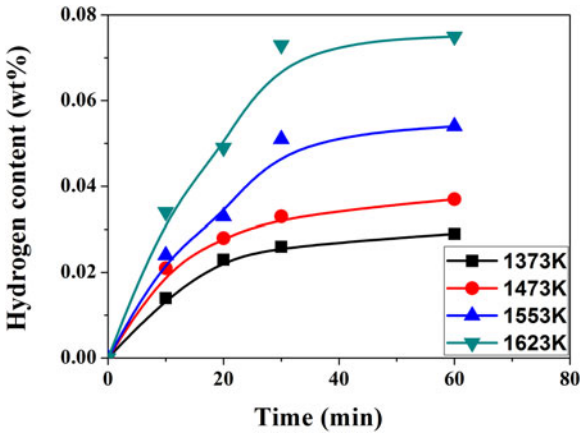


FIG. 5. Effects of hydrogenation time on hydrogen content for Ti–44Al–6Nb alloy.

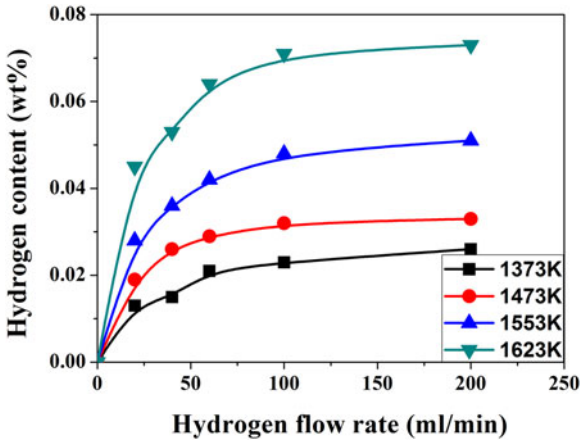


FIG. 6. Effect of hydrogen flow rate on hydrogen content at different temperatures for 30 min.

D. Effects of hydrogen on microstructure

The microstructures of unhydrogenated and hydrogenated Ti–44Al–6Nb alloys at different temperatures are shown in Fig. 7. The microstructures are influenced by temperature and hydrogen. The microstructure of unhydrogenated alloy and hydrogenated alloy is coarse dendritic structure which is similar to the as-cast alloy when treated below 1473 K. The duplex microstructure and block γ phase are not observed because of the low heating temperature and short holding time. The duplex microstructure of Ti–44Al–8Nb alloy is formed when soaking for 6 h at the 1553 K.[28] The microsegregation is eliminated partly during heating which will be discussed below. The effect of hydrogen on the lamellar colonies is not obvious at relative low temperature, such as at 1373 and 1473 K. When treated above 1553 K, the dendritic structure changes to equiaxed grain. The fully lamellar structure is obtained when cooled from single α region. The microstructure is usually characterized with coarse grains which are determined by heating temperature as shown in Fig. 7. The boundary of lamellar colonies for the hydrogenated alloy is smooth compared with the unhydrogeanted alloy as shown in Fig. 7. The α_2/γ lamellar is formed during continuous cooling from single α region by the reaction of $\alpha \rightarrow \alpha + \gamma \rightarrow \alpha_2 + \gamma$. The γ phase nucleates on Shockley dislocations and grows in the direction of $(0001)_\alpha$ as reported by Ramanujan.[29] The γ phase grows across the grain boundary and the zigzag interface is formed under large driving force.[30] Hydrogen decreases the interfacial energy by hydrogen-weakened bonds resulting in smooth grain boundary. The interface energy of TiAl/Ti_3Al interface is decreased by hydrogen using first-principles calculation method, which is attributed to the formation of the H–Ti and H–Al bonding after the addition of H at the interface.[31]

The size of lamellar colonies is statistically measured and the results are listed in Table II. The lamellar colony size is influenced by temperature, which increases with increasing of temperature up and down. The refined grains are obtained after isothermal heat treatment at 1553 K, which is above the T_α temperature a couple of degrees. The refined fully lamellar microstructure is obtained in Ti–46Al–2Cr–2Mo–0.25Si–0.3B alloy by heat-treatments which exploit the suppression of the $\alpha \rightarrow \alpha + \gamma$ transformation or involve cyclic annealing around the T_α.[32] When treated above T_α, the lamellar colonies grow with increasing of temperature; the lamellar colony size is 0.96 mm at 1553 K compared with that of 1.23 mm at 1623 K. The lamellar colonies grow rapidly because that the diffusion of elements is easy at elevated temperature and there is no barrier for grain growth when heat treatment is carried out in single α region.[33] The lamellar colony size is also influenced by hydrogen which promotes the lamellar colony size, such

https://doi.org/10.1557/jmr.2016.520 Published online by Cambridge University Press

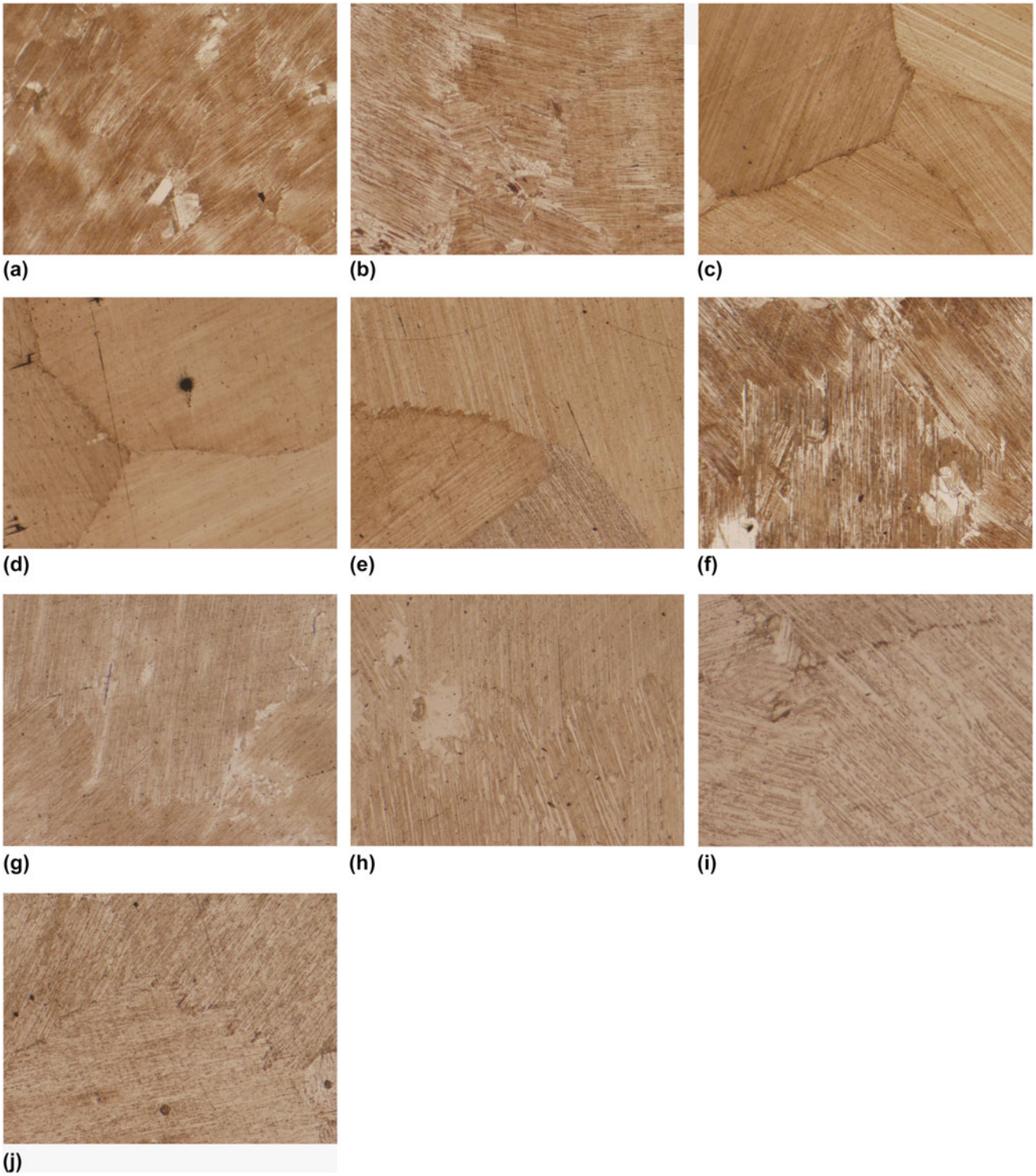


FIG. 7. Microstructure of unhydrogenated and hydrogenated Ti–44Al–6Nb alloys: (a) 1373 K/H, (b) 1473 K/H, (c) 1553 K/H, (d) 1623 K/H, (e) 1693 K/H, (f) 1373 K/Ar, (g) 1473 K/H/Ar, (h) 1553 K/Ar, (i) 1623 K/Ar, (j) 1693 K/Ar.

as the lamellar colony size of the unhydrogenated alloy and hydrogenated alloy is 0.96 and 1.04 mm at 1553 K respectively. The growth of lamellar colonies is controlled by diffusion during heat treatment at high temperature. Hydrogen weakens the bonds and decreases the energy barrier, which promotes the diffusion of elements, such as Al, Ti, V resulting in promoting the growth of grain. The first-principles calculation results

https://doi.org/10.1557/jmr.2016.520 Published online by Cambridge University Press

show that hydrogen can improves the Ti and Al self-diffusion coefficient and hydrogen enhanced the diffusion ability of alloy elements is also observed in diffusion bonding of TiAl-based alloys and Ti–6Al–4V interlayer.[34,35]

The effect of hydrogen on B2 phase was studied by SEM as shown in Fig. 8. The B2 phase in the unhydrogenated and hydrogenated alloys is still obvious after treating at 1473 K, while the residual B2 phase in hydrogenated alloy is more obvious than that of the unhydrogenated alloy. The B2 phase in the hydrogenated alloy is bone-like and is refined compared with that in the unhydrogenated alloy. The quantitative effect of hydrogen on B2 phase was studied by EDS and the results were shown in Table III. The Nb content in B2 phase is higher in the hydrogenated alloy than that in unhydrogenated alloy. This is because that hydrogen is strong beta stabilizing element which stabilizes B2 phase during hydrogenation. Wen studied the effect of hydrogen on phase transformation of Ti–45Al–5Nb–0.8Mo–0.3Y alloy during hot deformation, and found that the volume fraction of B2 phase of the hydrogenated alloy was larger than that of the unhydrogenated alloys using EBSD method, which was well agreed with this study.[36] Schmoelzer studied the transition of phase fraction of TiAl–Nb–Mo alloys by in situ high energy synchrotron X-ray diffraction, the results showed that the volume fraction of B2 phase increased with increasing of beta stabilizing elements.[37] The Nb content and Al content in the lamellar of the hydrogenated alloy is more homogeneous compared with that of unhydrogenated alloy. It is considered that hydrogen promotes the diffusion of Ti and Al, consequently the segregation of Ti and Al is partly eliminated.

The effect of hydrogen on lamellar spacing is studied using TEM as shown in Fig. 9. The lamellar spacing of the unhydrogenated alloy and hydrogenated alloy is 875 and 1070 nm respectively. It is revealing that hydrogen promotes the coarsening of lamellar spacing. The coarsening of lamellar spacing is a process of diffusion and hydrogen promotes the Ti and Al self-diffusion coefficient resulting in promoting the coarsening of lamellar spacing. The B2 phase and hydride are not observed in the unhydrogenated and hydrogenated alloys by TEM. This is because that the content of B2 phase is low and partly dissolves in the matrix.

The XRD results of unhydrogenated and hydrogenated alloys are shown in Fig. 10. The unhydrogenated alloy and hydrogenated alloy are composed of α_2 phase, γ phase, and B2 phase. The diffraction peak position is not changed after hydrogenation, while the diffraction peak intensity of γ phase in the hydrogenated alloy is more than that in unhydrogenated alloy. More γ phase is formed after hydrogenation. Hydrogen is beta stabilizing elements, addition of hydrogen changes the diagram to the high Al content and consequently more γ phase is obtained in TiAl alloys. Clemens[38] reported that addition of Mo beta stabilizing elements in TiAl alloys resulting in the increase of γ phase. The hydride is not detected in hydrogenated alloy. Hydrides are not observed in TiAl alloys after gaseous hydrogen charging at high temperature (300–973 K) and high pressure (0.1–10 MPa) by

TABLE II. Lamellar colony size of unhydrogenated and hydrogenated alloys under different temperatures.

	Lamellar colony size (mm)				
Alloys	1373 K	1473 K	1553 K	1623 K	1693 K
Hydrogenated alloy	1.07	1.14	1.04	1.31	1.49
Unhydrogenated alloy	1.04	1.09	0.96	1.23	1.35

TABLE III. EDS results of the hydrogenated alloy and unhydrogenated alloy.

Element	A point (at.%)	B point (at.%)	C point (at.%)	D point (at.%)
AlK	47.98	42.47	50.26	47.47
TiK	46.54	50.41	47.42	46.36
Nb	5.49	7.11	2.32	6.17

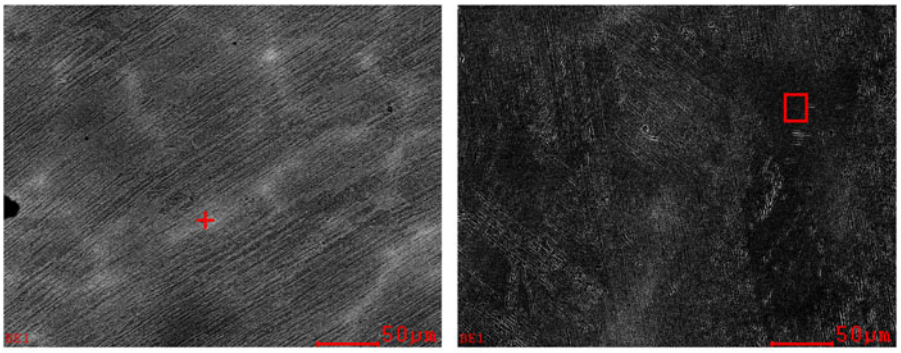


FIG. 8. Microstructure of Ti–44Al–6Nb alloy at 1473 K: (a) hydrogenated alloy, (b) unhydrogenated alloy.

https://doi.org/10.1557/jmr.2016.520 Published online by Cambridge University Press

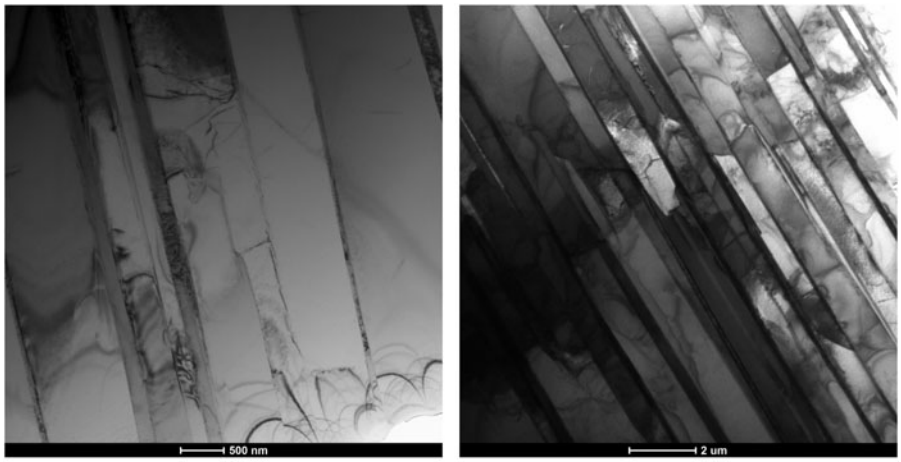


FIG. 9. The lamellar structure of Ti–44Al–6Nb alloy treated at 1473 K: (a) unhydrogenated alloy, (b) hydrogenated alloy.

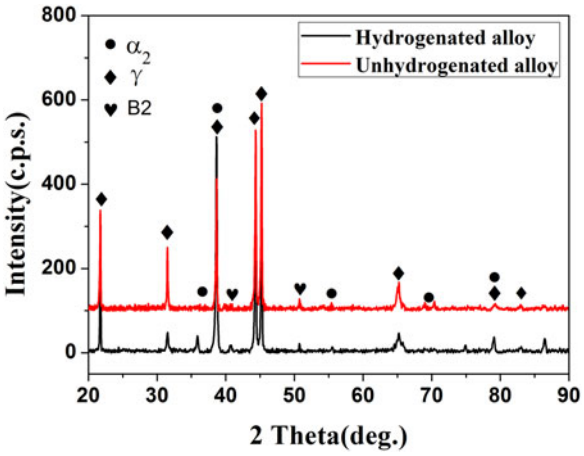


FIG. 10. XRD results of unhydrogenated and hydrogenated Ti–44Al–6Nb alloys at 1473 K.

Zong and A. Takasaki.[13,36] While P.A. Sundaram found the hydrides in Ti–48Al–2Cr and Ti–46.5Al–4(Cr, Nb, Ta, B) alloys after electrolytic charging based on the hydrogen effusion experiments.[39] It is considered that the charging method has a directed effect on the formation of hydrides.

E. Effect of hydrogen on mechanical properties

The nanohardness and elastic modulus of the unhydrogenated and hydrogenated Ti–44Al–6Nb alloys are listed in Table IV. The hydrogenated alloy is the alloy hydrogenated with the maximum hydrogen content 0.033 wt% H. The nanohardness of the hydrogenated alloy is 4.2 GPa compared with that of 4.4 GPa for unhdyrogenated alloy, and the elastic modulus of Ti–44Al–6Nb alloy is decreased from 213.5 to 199.8 GPa after hydrogenated with 0.033 wt% H. The hardness is inversely proportional to lamellar spacing,

TABLE IV. Nanohardness and elastic modulus of unhydrogenated and hydrogenated Ti–44Al–6Nb alloys at 1473 K.

Condition	Nanohardness/GPa	Elastic modulus/GPa
Hydrogenated alloy	4.2	199.8
Unhydrogenated alloy	4.4	213.5
Hydrogenated Ti–46.5Al–4(Cr, Nb, Ta, B)	2.7	83
Unhydrogenated Ti–46.5Al–4(Cr, Nb, Ta, B)	3.0	140

that is to say the hardness decreases with increasing of lamellar spacing. The lamellar spacing of hydrogenated alloy is larger than that of unhydrogenated alloy resulting in lower nanohardness. The effect of hydrogen on hardness and elastic modulus of Ti–46.5Al–4(Cr, Nb, Ta, B) alloy is also listed in Table IV for comparison.[40] The values of hardness and elastic modulus obtained in this study are larger than that in reference due to the different test methods, microstructures and alloy compositions. The effect of hydrogen on elastic modulus is studied by first-principles calculation, the results show that the hydrogen can reduce the elastic modulus of TiAl alloys and the interstitial sites hydrogen occupied has a great effect on elastic modulus.[23] It is considered that a certain amount of hydrogen weakens the bonds in TiAl alloys causing a reduction of elastic modulus.

The true stress–strain curves of Ti–44Al–6Nb alloys hydrogenated with different hydrogen content after thermal simulation are partly shown in Fig. 11(a). The flow curves exhibit the work hardening at the initial deformation stage and dynamic recrystallization softening with the increasing of strain. The flow stress increase firstly and reaches to the maximum, then decreases continuously and reaches a steady state with increasing strain. The similar flow feature is also observed in TiAl alloys

https://doi.org/10.1557/jmr.2016.520 Published online by Cambridge University Press

hot deformation at temperature range of 1373–1523 K and strain rate of 0.001–1 s^{-1} by Lin.[41] The peak stress dependence on the hydrogen content at various deformation temperatures is shown in Fig. 11(b). The peak stress decreases with the increase of temperature and hydrogen content. The peak stress of the unhydrogenated alloy and hydrogenated alloy is 307 and 214 MPa respectively, which is decreased by 30% deformed at 1423 K. The peak stress of unhydrogeanted alloy deformed at 1473 K is 233 MPa suggesting that 0.033 wt% H can decrease the deformation temperature by about 50 K. Hydrogen-induced decrease of flow stress is also reported in titanium alloy, α_2-based alloys and TiAl alloys, such as addition of 0.5 wt% hydrogen in Ti40 alloy can decrease the flow stress by 35%, the peak stress of Ti–25Al–l0Nb–3V–lMo alloy is decreased by 31% after addition of 0.2 wt% H, the peak stress of Ti–47Al alloy is reduced by about 33.3% with 0.027 wt% H.[10,25,42] Hydrogen-induced decrease

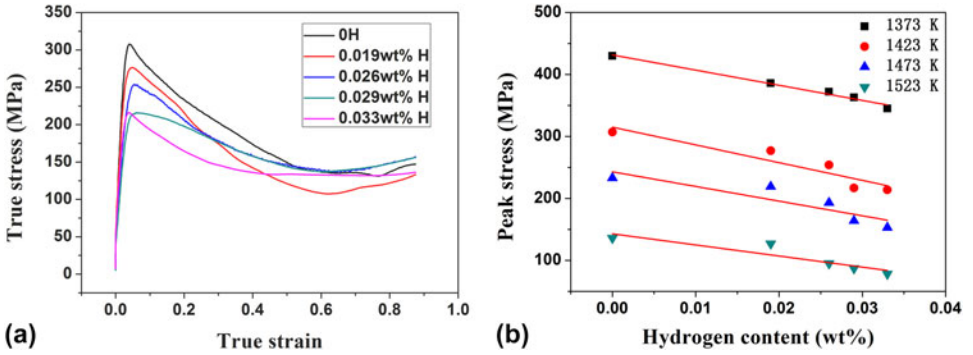


FIG. 11. Hot compressive results of Ti–44Al–6Nb alloy with different hydrogen content: (a) the effect of hydrogen content on true stress–strain curves, (b) the peak stress versus hydrogen content.

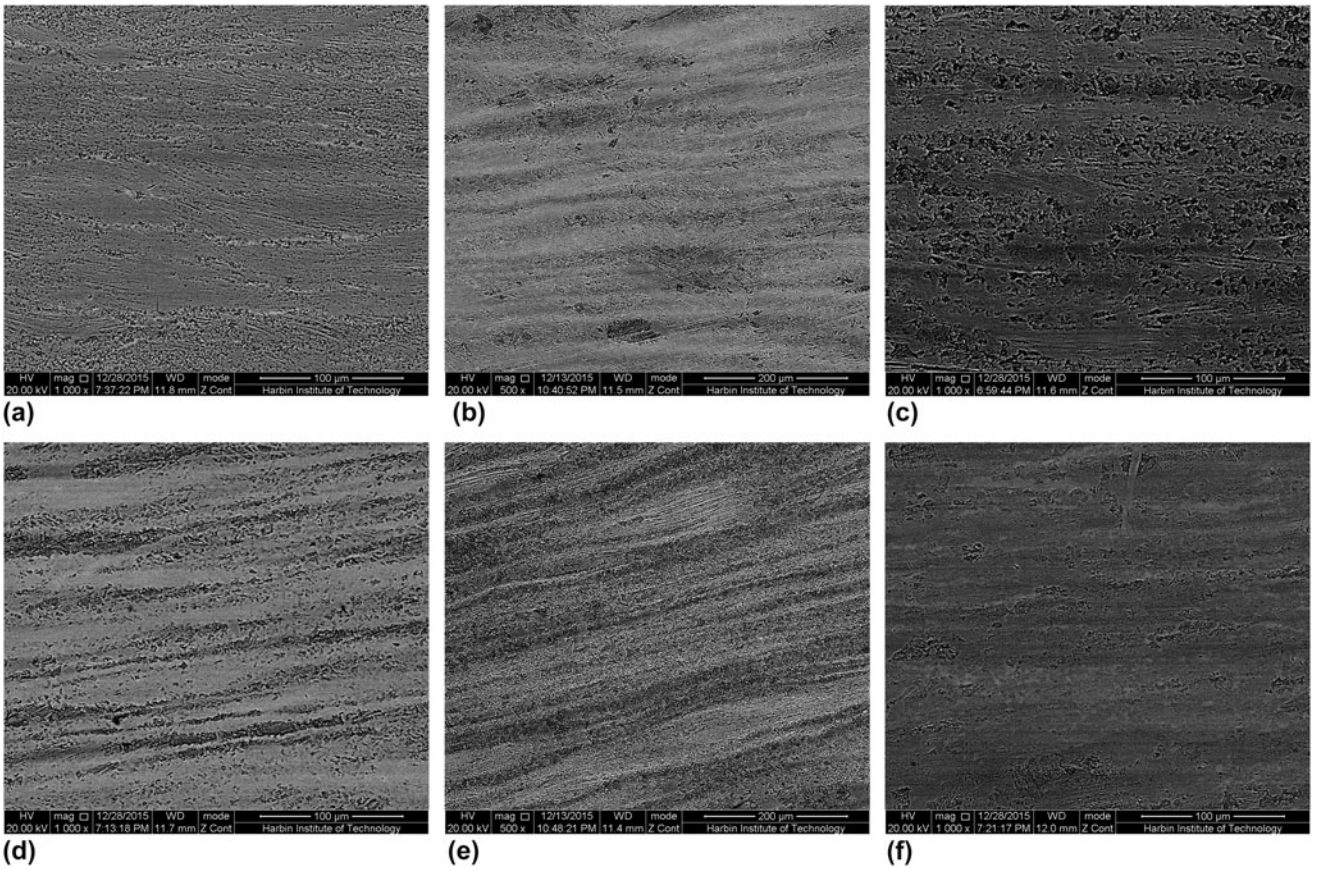


FIG. 12. Deformation microstructures of unhydrogenated alloy [(a)–(c)] and hydrogenated alloy [(d)–(f)] at different temperatures under strain rate of 0.01 s^{-1}: (a), (d)1423 K, (b), (e)1473 K, (c), (f)1523 K.

https://doi.org/10.1557/jmr.2016.520 Published online by Cambridge University Press

of flow stress is attributed to hydrogen promotes the dislocation movement and dynamic recrystallization, which will be studied systematically below. The flow stress of steel is also reduced by interstitial atoms such as boron and carbon, the flow stress of plain carbon steel is decreased by 12% with addition of 1.25 wt% carbon reported by Wray, a solid solution softening effect of boron is also observed in ultrahigh strength steels by Mejía.[43,44]

The deformation microstructures of unhydrogenated and hydrogenated alloys are shown in Fig. 12. The deformation microstructures of unhydrogenated and hydrogenated alloys are composed of elongated lamellar colonies (remnant lamellar RL) and dynamic recrystallization (DRX) grains. When deformation temperature is low, the lamellar colony is elongated along the deformation direction, the band structure is formed as shown in Fig. 12(a). The DRX grains are formed around the lamellar colony boundaries where the stored energy and dislocation density are high. The DRX of TiAl alloys is discontinuous dynamic recrystallization involving nucleation and growth of DRX grains due to the low stacking energy. The degree of DRX increases with increasing of temperature and the volume fraction of DRX grains is enhanced as shown in Figs. 12(a)–12(c). The degree of DRX in hydrogenated alloy is more obvious than that in unhydrogenated alloy at the same deformation temperature as shown in Figs. 12(a) and 12(c). That is to say, hydrogen promotes the DRX of TiAl alloys. By comparing with the deformation microstructure, the deformation temperature is decreased by about 50 K after hydrogenation. Hydrogen-promoted the DRX are mainly attributed to hydrogen promoting decomposition of α_2/γ lamellar and nucleation and growth of DRX grains.[45] DRX is the main softening mechanism of TiAl alloys, hydrogen promotes the DRX and leads to the decrease of flow stress as shown in Fig. 11.

The TEM micrographs of unhydrogenated and hydrogenated alloys are shown in Fig. 13. The typical

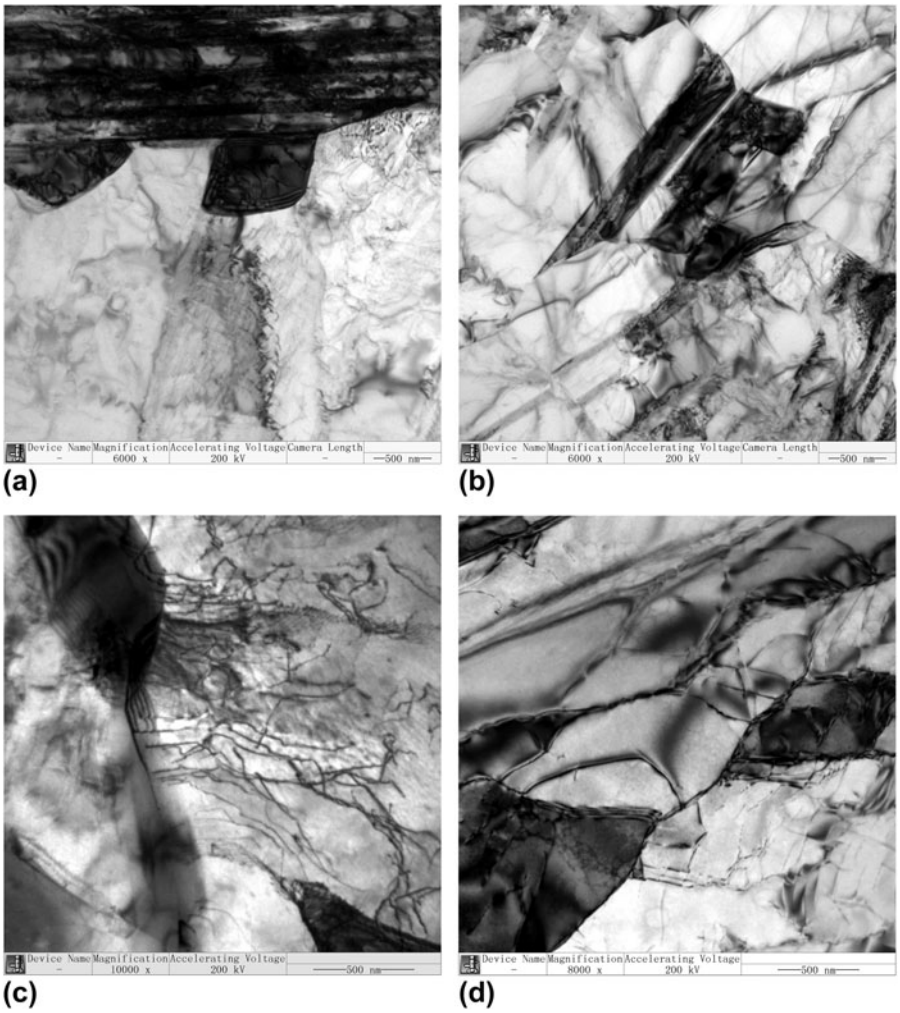


FIG. 13. The deformation microstructure of unhydrogenated and hydrogenated Ti–44Al–6Nb alloys deformed at 1473 K under strain rate of 0.01 s^{-1}: (a), (b) unhydrogenated alloy, (c), (d) hydrogenated alloy.

https://doi.org/10.1557/jmr.2016.520 Published online by Cambridge University Press

deformation microstructures of TiAl alloys are RL microstructure and DRX grains. The dislocation tangles are obvious in the unhydrogenated alloy and hydrogenated alloy indicating that dislocation movement is another softening mechanism of TiAl alloys. The more dislocation tangles are observed in RL region of unhydrogenated alloy compared with that of the hydrogenated alloy, which denotes that hydrogen can promote the dislocation movement. Hydrogen-induced the decrease of the dislocation tangles and dislocation density has been observed in Ti–6Al–4V alloy and TiAl alloys.[9,11] Dislocation tangles are also observed in some DRX grains revealing that the DRX grains are suffering deformation. As a result, the flow stress can be decreased further. The DRX grains nucleate on the lamellar colony boundary as shown in Fig. 13(a). The degree of DRX in the hydrogenated alloy is higher than that in unhydrogenated alloy, and more DRX grains are observed in hydrogenated alloy. The size of DRX grains in hydrogenated alloy is larger than that in the unhydrogenated alloy. Hydrogen promotes the nucleation of TiAl alloys by promoting the decomposition of lamellar colonies, and more nucleation sites are obtained as reported by Zong.[45] Hydrogen can also decrease the interface energy resulting in the decrease of critical nucleation energy. Hydrogen promotes the diffusion of elements and then the grain boundary migration rate can be accelerated. Consequently, the more and larger DRX grains are formed in the hydrogenated alloy resulting in low flow stress and peak stress.

IV. CONCLUSIONS

The Ti–44Al–6Nb alloy was hydrogenated at temperature range of 1373–1693 K, and the effect of hydrogen on its microstructure and hot deformability was studied, the following conclusions can be obtained:

(1) The relationship between hydrogen content and hydrogenation temperature can be expressed as: $C_H = 25.44\exp\left(-9.792\times10^3/T\right)$, where the heat of solution of hydrogen in Ti–44Al–6Nb alloy is calculated as 81.4 kJ/mol. The positive value of the heat of solution of hydrogen reveals that hydrogen absorption in TiAl alloys is endothermic and hydrogen content increases with increasing of temperature.

(2) Hydrogen promotes the lamellar colony size and lamellar spacing by promoting the diffusion of alloy elements, and stabilizes B2 phase during high temperature hydrogenation because that hydrogen is beta stabilizing element.

(3) The nanohardness and elasticity modulus of Ti–44Al–6Nb alloy are reduced after hydrogenation, which is attributed to hydrogen-weakened bonds and the coarsening of lamellar spacing.

(4) Hydrogen can obviously decrease the peak stress of TiAl alloys which can be decreased by 30% at most, corresponding to decreasing the deformation temperature by about 50 K based on the peak stress and deformation microstructure. This is attributed to hydrogen-promoted the dynamic recrystallization and dislocation movement.

ACKNOWLEDGMENTS

This work was supported by National Natural Science Foundation of China (51274076) and The National Science Fund for Distinguished Young Scholars (NSFC51425402).

REFERENCES

1. N. Cinca, C.R.C. Lima, and J.M. Guilemany: An overview of intermetallics research and application: Status of thermal spray coatings. *J. Mater. Sci. Technol.* **2**, 75 (2013).
2. B. Liu, Y. Liu, C. Qiu, C. Zhou, J. Li, H. Li, and Y. He: Design of low-cost titanium aluminide intermetallics. *J Alloys Compd.* **640**, 298 (2015).
3. Y. Xia, P. Yu, G.B. Schaffer, and M. Qian: Cobalt-doped Ti–48-Al–2Cr–2Nb alloy fabricated by cold compaction and pressureless sintering. *Mater. Sci. Eng., A* **574**, 176 (2013).
4. F. Kong, N. Cui, Y. Chen, X. Wang, and N. Xiong: Characterization of hot deformation behavior of as-forged TiAl alloy. *Intermetallics* **55**, 66 (2014).
5. R. Gerling, A. Bartels, H. Clemens, H. Kestler, and F. Schimansky: Structural characterization and tensile properties of a high niobium containing gamma TiAl sheet obtained by powder metallurgical processing. *Intermetallics* **12**, 275 (2004).
6. F.H. Froes, O.N. Senkov, and J.I. Qazi: Hydrogen as a temporary alloying element in titanium alloys: Thermohydrogen processing. *Int. Mater. Rev.* **49**, 227 (2004).
7. N. Eliaz, D. Eliezer, and D.L. Olson: Hydrogen-assisted processing of materials. *Mater. Sci. Eng., A* **289**, 41 (2000).
8. O.N. Senkov and F.H. Froes: Thermohydrogen processing of titanium alloys. *Int. J. Hydrogen Energy* **24**, 565 (1999).
9. Y. Zong, D. Shan, Y. Lv, and B. Guo: Effect of 0.3 wt% H addition on the high temperature deformation behaviors of Ti–6Al–4V alloy. *Int. J. Hydrogen Energy* **32**, 3936 (2007).
10. X. Liu, Y. Su, L. Luo, J. Liu, J. Guo, and H. Fu: Effect of hydrogen on hot deformation behaviors of TiAl alloys. *Int. J. Hydrogen Energy* **35**, 13322 (2010).
11. D.S. Wen, Y.Y. Zong, Y.Q. Wang, Z.Y. Liu, and D.B. Shan: Positive influence of hydrogen on the hot workability and dynamic recrystallization of a γ-TiAl based alloy. *Mater. Sci. Eng., A* **656**, 151 (2016).
12. A. Takasaki, Y. Furuya, K. Ojima, and Y. Taneda: Hydrogen solubility of two-phase (Ti_3Al + TiAl) titanium aluminides. *Scr. Mater.* **32**, 1759 (1995).
13. A. Takasaki, Y. Furuya, and Y. Taneda: Hydrogen uptake in titanium aluminides in high pressure hydrogen. *Mater. Sci. Eng., A* **239–240**, 265 (1997).
14. A. Takasaki: High-pressure hydrogen charging of TiAl-based titanium aluminides. *Scr. Mater.* **38**, 687 (1998).
15. J.X. Zhang and H.Q. He: Deformation-induced γ → DI-α2 phase transformation in a Ti–48Al–2Cr alloy. *J. Mater. Res.* **15**, 2145 (2000).
16. S.R. Dey, E. Bouzy, and A. Hazotte: Intragranular nucleation sites of massive γ grains in a TiAl-based alloy. *Scr. Mater.* **57**, 365 (2007).
17. Y. Li, L. Zhou, J. Lin, H. Chang, and F. Li: Phase transformation behavior and kinetics of high Nb–TiAl alloy during continuous cooling. *J Alloys Compd.* **668**, 22 (2016).

https://doi.org/10.1557/jmr.2016.520 Published online by Cambridge University Press

18. J.P. Cui, M.L. Sui, Y.Y. Cui, and D.X. Li: Ductile TiAl alloy with a widmanstatten lamellar structure formed by rapid heating. *J. Mater. Res.* **23**, 949 (2008).
19. J.I. Qazi, O.N. Senkov, J. Rahim, A. Genc, and F.H. Froes: Phase transformations in Ti6Al4V–xH alloys. *Metall. Mater. Trans. A* **32A**, 2453 (2001).
20. G. Liu, X. Li, Y. Su, D. Liu, J. Guo, and H. Fu: Microstructure, microsegregation pattern and the formation of B2 phase in directionally solidified Ti–46Al–8Nb alloy. *J Alloys Compd.* **541**, 275 (2012).
21. T. Voisin, J. Monchoux, M. Hantcherli, S. Mayer, H. Clemens, and A. Couret: Microstructures and mechanical properties of a multi-phase β-solidifying TiAl alloy densified by spark plasma sintering. *Acta Mater.* **73**, 107 (2014).
22. H.F. Chladil, H. Clemens, H. Leitner, A. Bartels, R. Gerling, F.P. Schimansky, and S. Kremmer: Phase transformations in high niobium and carbon containing γ-TiAl based alloys. *Intermetallics* **14**, 1194 (2006).
23. S. Chen, C.P. Liang, and H.R. Gong: Structural stability, mechanical property and elastic anisotropy of TiAl-H system. *Int. J. Hydrogen Energy* **37**, 2676 (2012).
24. M. Niinomi, B. Gong, T. Kobayashi, Y. Ohyabu, and O. Toriyama: Fracture characteristics of Ti–6Al–4V and Ti–5Al–2.5Fe with refined microstructure using hydrogen. *Metall. Mater. Trans. A* **26**, 1141 (1995).
25. Y. Zhang, S.Q. Zhang, and C. Tao: Hydrogenation behavior of Ti–25Al–l0Nb–3V–1Mo and effect of hydrogen on its microstructure deformability. *Int. J. Hydrogen Energy* **22**, 125 (1997).
26. P.A. Sundaram, E. Wessel, H. Clemens, H. Kestler, and P.J. Ennis: Determination of the diffusion coefficient of hydrogen in gamma titanium aluminides during electrolytic charging. *Acta Mater.* **48**, 1005 (2000).
27. Y. Su, X. Liu, L. Luo, L. Zhao, J. Guo, and H. Fu: Hydrogen solubility in molten TiAl alloys. *Int. J. Hydrogen Energy* **35**, 8008 (2010).
28. A. Huang, D. Hu, M.H. Loretto, J. Mei, and X. Wu: The influence of pressure on solid-state transformations in Ti–46Al–8Nb. *Scr. Mater.* **56**, 253 (2007).
29. R.V. Ramanujan: Phase transformations in γ based titanium aluminides. *Int. Mater. Rev.* **45**, 217 (2000).
30. F.T. Kong, S.L. Xiao, Y.Y. Chen, and B.H. Li: Continuous cooling chase transformation of Ti–45Al–5Nb(–0.3Y) alloys. *Rare Metal. Mat. Eng.* **38**, 25 (2009).
31. Y. Wei, Y. Zhang, G. Lu, and H. Xu: A first-principles study of site occupancy and interfacial energetics of an H-doped TiAl–Ti_3Al alloy. *Sci. China Phys. Mech.* **55**, 228 (2012).
32. H. Clemens, A. Bartels, S. Bystrzanowski, H. Chladil, H. Leitner, G. Dehm, R. Gerling, and F.P. Schimansky: Grain refinement in γ-TiAl-based alloys by solid state phase transformations. *Intermetallics* **14**, 1380 (2006).
33. S. Dong, R. Chen, J. Guo, H. Ding, Y. Su, and H. Fu: Effect of heat treatment on microstructure and mechanical properties of cast and directionally solidified high-Nb contained TiAl-based alloy. *J. Mater. Res.* **30**, 3331 (2015).
34. X.L. Han, Q. Wang, D.L. Sun, and H.X. Zhang: First-principles study of the effect of hydrogen on the Ti self-diffusion characteristics in the alpha Ti–H system. *Scr. Mater.* **56**, 77 (2007).
35. P. He, L. Fan, H. Liu, and J.C. Feng: Effects of hydrogen on diffusion bonding of TiAl-based intermetallics using hydrogenated Ti6Al4V interlayer. *Int. J. Hydrogen Energy* **35**, 13317 (2010).
36. D. Wen, Y. Zong, W. Xu, D. Shan, and B. Guo: The effect of hydrogen on phase transformation and mechanical properties of a β containing γ–TiAl based alloy. *Int. J. Hydrogen Energy* **39**, 17404 (2014).
37. T. Schmoelzer, K. Liss, G.A. Zickler, I.J. Watson, L.M. Droessler, W. Wallgram, T. Buslaps, A. Studer, and H. Clemens: Phase fractions, transition and ordering temperatures in TiAl–Nb–Mo alloys: An *in-* and *ex-situ* study. *Intermetallics* **18**, 1544 (2010).
38. H. Clemens, W. Wallgram, S. Kremmer, V. Güther, A. Otto, and A. Bartels: Design of novel β-solidifying TiAl alloys with adjustable β/B2-Phase fraction and excellent hot-workability. *Adv. Eng. Mater.* **10**, 707 (2008).
39. P.A. Sundaram, W.J. Quadakkers, and L. Singheiser: Hydrogen effusion in cathodically charged gamma titanium aluminides. *J Alloys Compd.* **298**, 274 (2000).
40. P.A. Sundaram, D. Basu, R.W. Steinbrech, P.J. Ennis, W.J. Quadakkers, and L. Singheiser: Effect of hydrogen on the elastic modulus and hardness of gamma titanium aluminides. *Scr. Mater.* **41**, 839 (1999).
41. X.J. Xu, J.P. Lin, Y.L. Wang, Z. Lin, and G.L. Chen: Deformability and microstructure transformation of pilot ingot of Ti–45Al–(8–9)Nb–(W, B, Y) alloy. *Mater. Sci. Eng., A.* **416**, 98 (2006).
42. W.J. He, S.H. Zhang, H.W. Song, and M. Cheng: Hydrogen-induced hardening and softening of a β-titanium alloy. *Scr. Mater.* **61**, 16 (2009).
43. P.J. Wray: Effect of carbon content on the plastic flow of plain carbon steels at elevated temperatures. *Metall. Mater. Trans. A* **13**, 125 (1982).
44. I. Mejía, G. Altamirano, A. Bedolla-Jacuinde, and J.M. Cabrera: Modeling of the hot flow behavior of advanced ultra-high strength steels (A-UHSS) microalloyed with boron. *Mater. Sci. Eng., A* **610**, 116 (2014).
45. Y.Y. Zong, D.S. Wen, Z.Y. Liu, and D.B. Shan: Effect of hydrogen on the microstructural evolution of a γ-TiAl based alloy. *Mater. Lett.* **14**, 223 (2015).

https://doi.org/10.1557/jmr.2016.520 Published online by Cambridge University Press